Inorg. Chem. **2002**, *41*, 6372–6379

Salt-Free Synthesis of Samarium–Aluminum Mixed-Metal Alkoxides: X-ray Crystal Structures of $\{[(i\text{-Pr-O})(i\text{-Bu})Al(\mu\text{-O-}i\text{-Pr})_2Sm(O\text{-}i\text{-Pr})(HO\text{-}i\text{-Pr})](\mu\text{-O-}i\text{-Pr})\}_2$, $[(THF)_2Sm(O\text{-}t\text{-Bu})_2(\mu\text{-O-}t\text{-Bu})_2Al(i\text{-Bu})_2]$, $Sm(OAr)_3(THF)_3$ (Ar = 2,4,6-$Me_3C_6H_2$), $[Nd(\mu\text{-OAr})(OAr)_2(py)_2]_2$ (Ar = 2,4,6-$Me_3C_6H_2$), and $(ArO)_3Sm[(\mu\text{-O-}t\text{-Bu})_2Al_2(O\text{-}t\text{-Bu})_4]$ (Ar = 2,6-i-$Pr_2C_6H_3$)

Garth R. Giesbrecht,[1a] John C. Gordon,*[,1b] David L. Clark,[1c] Brian L. Scott,[1b] John G. Watkin,*[,1b] and Kenneth J. Young[1b]

Nuclear Materials Technology (NMT) Division, Chemistry (C) Division, and the Glenn T. Seaborg Institute for Transactinium Science, Los Alamos National Laboratory, Los Alamos, New Mexico 87545

Received May 3, 2002

Reaction of equimolar quantities of $Sm[N(SiMe_3)_2]_3$ and $Al(i\text{-Bu})_3$ with 6 equiv of *iso*-propyl alcohol in toluene leads to the formation of the mixed-metal alkoxide complex $\{[(i\text{-Pr-O})(i\text{-Bu})Al(\mu\text{-O-}i\text{-Pr})_2Sm(O\text{-}i\text{-Pr})(HO\text{-}i\text{-Pr})](\mu\text{-O-}i\text{-Pr})\}_2$ (**1**). An analogous reaction between 1:1 $Sm[N(SiMe_3)_2]_3/Al(i\text{-Bu})_3$ and 6 equiv of *tert*-butyl alcohol, followed by addition of THF, produces the THF adduct $[(THF)_2Sm(O\text{-}t\text{-Bu})_2(\mu\text{-O-}t\text{-Bu})_2Al(i\text{-Bu})_2]$ (**2**). Compound **1** crystallizes in the space group $P\bar{1}$ while **2** crystallizes in space group *Cmcm*. Cell parameters for **1**: $a = 11.028(2)$ Å, $b = 12.168(2)$ Å, $c = 12.879(2)$ Å, $\alpha = 82.84(1)°$, $\beta = 64.88(1)°$, $\gamma = 70.80(1)°$, $Z = 1$. Cell parameters for **2**: $a = 11.304(2)$ Å, $b = 22.429(4)$ Å, $c = 15.768(2)$ Å, $Z = 4$. Attempts to prepare the bulkier derivatives result in the formation of lanthanide aryloxide species only; reaction between equimolar amounts of $Ln[N(SiMe_3)_2]_3$ (Ln = Sm, Nd) and $Al(i\text{-Bu})_3$ with 6 equiv of HO-2,4,6-$Me_3C_6H_2$, followed by the addition of THF or pyridine, yields the Lewis base adducts $Sm(OAr)_3(THF)_3$ (**3**) and $[Nd(\mu\text{-OAr})(OAr)_2(py)_2]_2$ (**4**). Compound **3** crystallizes in the space group *Pbca* while **4** crystallizes in space group $P2_1/c$. Cell parameters for **3**: $a = 16.5822(9)$ Å, $b = 15.5668(9)$ Å, $c = 29.902(2)$ Å, $Z = 8$. Cell parameters for **4**: $a = 13.4496(8)$ Å, $b = 20.034(1)$ Å, $c = 16.206(1)$ Å, $\beta = 113.782(1)°$, $Z = 2$. Reaction of $Al_2(O\text{-}t\text{-Bu})_6$ with $[Sm(OAr)_3]_2$ (Ar = 2,6-i-$Pr_2C_6H_3$) yields the adduct $(ArO)_3Sm[(\mu\text{-O-}t\text{-Bu})_2Al_2(O\text{-}t\text{-Bu})_4]$ (**5**), which crystallizes in the space group $P2_1/n$. Cell parameters for **5**: $a = 14.0960(7)$ Å, $b = 27.3037(15)$ Å, $c = 16.7893(9)$ Å, $\beta = 92.216(1)°$, $Z = 4$.

Introduction

In recent years, the preparation of metal alkoxide complexes for use in the sol–gel synthesis of metal oxide materials has become an area of considerable research interest.[2–6] In addition to its utility in the preparation of metal oxide phases containing a single metal, the sol–gel process has also been utilized to prepare mixed-metal oxides, either by sol–gel processing of a mixture of two metal alkoxides in the desired stoichiometric ratio, or by processing of a single-source mixed-metal alkoxide.[7–11] The synthesis of mixed-metal lanthanide–aluminum alkoxides as precursors to lanthanide-doped alumina appears to be an attractive area

* To whom correspondence should be addressed. E-mail: jgordon@lanl.gov.

(1) (a) NMT-DO, Mail Stop J514. (b) C-SIC, Mail Stop J514. (c) G. T. Seaborg Institute, Mail Stop E500.
(2) Spiccia, L.; Watkins, I. D.; West, B. O. *Materials Forum* **1996**, *20*, 171.
(3) Schubert, U.; Huesing, N.; Lorenz, A. *Chem. Mater.* **1995**, *7*, 2010.
(4) Mehrotra, R. C. *Proc. Int. Symp. Adv. Sol–Gel Process. Appl.* **1994**, 41.
(5) Livage, J. *Mater. Sci. Forum* **1994**, *152–153*, 43.
(6) James, P. F. *Proc. Eur. Conf. Adv. Mater. Processes, 2nd* **1992**, *3*, 189.
(7) Mehrotra, R. C.; Singh, A.; Sogani, S. *Chem. Rev.* **1994**, *94*, 1643.
(8) Mehrotra, R. C. *J. Indian Chem. Soc.* **1994**, *71*, 315.
(9) Hubert-Pfalzgraf, L. G. *New J. Chem.* **1987**, *11*, 663.
(10) Hubert-Pfalzgraf, L. G. *Mater. Eng. (N.Y.)* **1994**, *8*, 23.
(11) Hubert-Pfalzgraf, L. G. *New J. Chem.* **1995**, *19*, 727.

10.1021/ic0203116 CCC: $22.00
Published on Web 11/05/2002

for study. Current applications of lanthanide-doped alumina include preparing phosphors for display panels,[12] synthesizing doped ceramic materials,[13] and increasing the catalytic activity of alumina-supported platinum catalysts,[14] while lanthanide-doped aluminum phosphate films are currently under study for their applicability in optical devices.[15,16] Previously described examples of mixed-metal lanthanide−aluminum alkoxides include the lanthanide(II) complexes $Ln[Al_3(O\text{-}i\text{-}Pr)_{11}]$ (Ln = Sm, Yb)[17] and the lanthanide(III) species $Ln[Al(O\text{-}i\text{-}Pr)_4]_3$ (Ln = Y, La, Pr, Nd, Sm, Dy, Yb),[18] $Er[Al(O\text{-}i\text{-}Pr)_4]_3$,[19] and $\{Pr[Al(O\text{-}i\text{-}Pr)_4]_2(Pr\text{-}i\text{-}OH)(\mu\text{-}Cl)\}_2$.[20] In related studies, we and others have described structural and spectroscopic investigations of a number of complexes resulting from the interaction of lanthanide alkoxide and aryloxides with trialkylaluminum reagents, for example, $(Bu\text{-}t\text{-}O)(THF)Y[(\mu\text{-}O\text{-}t\text{-}Bu)(\mu\text{-}Me)AlMe_2]_2$,[21] $(Bu\text{-}t\text{-}O)(Cl)(THF)_2Y(\mu\text{-}O\text{-}t\text{-}Bu)_2AlMe_2$,[21] $[Ln(\mu\text{-}O\text{-}t\text{-}Bu)_3(\mu\text{-}Me)_3(AlMe_2)_3]$ (Ln = Y, Pr, Nd),[22] $(ArO)Sm[\mu\text{-}OAr)(\mu\text{-}R)AlR_2]_2$ (Ar = 2,6-i-$Pr_2C_6H_3$, R = Me, Et),[23,24] and $(ArO)La[\mu\text{-}OAr)(\mu\text{-}Me)AlMe_2]_2$.[24]

It has been reported that mixed-metal alkoxide syntheses which employ halide metathesis techniques can allow incorporation of impurities such as alkali-metal cations or halide anions into the product.[25] Thus, we have investigated the synthesis of mixed-metal alkoxide species via alcoholysis of stoichiometric mixtures of metal amides and alkyls: the only byproducts from these reactions are volatile hydrocarbons or amines which may readily be removed by application of vacuum.

Results and Discussion

Alcoholysis of a mixture of the samarium tris(amido) complex, $Sm[N(SiMe_3)_2]_3$, and the trialkylaluminum reagent, $Al(i\text{-}Bu)_3$, was found to be a viable, although low yielding, synthetic route to the mixed-metal alkoxide complexes $\{[(i\text{-}Pr\text{-}O)(i\text{-}Bu)Al(\mu\text{-}O\text{-}i\text{-}Pr)_2Sm(O\text{-}i\text{-}Pr)(HO\text{-}i\text{-}Pr)](\mu\text{-}O\text{-}i\text{-}Pr)\}_2$ (**1**) and $[(THF)_2Sm(O\text{-}t\text{-}Bu)_2(\mu\text{-}O\text{-}t\text{-}Bu)_2Al(i\text{-}Bu)_2]$ (**2**) (eqs 1 and 2).

$$Sm[N(SiMe_3)_2]_3 + Al(i\text{-}Bu)_3 \xrightarrow[\text{toluene}]{6i\text{-Pr-OH}} \underset{\mathbf{1}}{[Sm(O\text{-}i\text{-}Pr)_3(HO\text{-}i\text{-}Pr)Al(O\text{-}i\text{-}Pr)_2(i\text{-}Bu_2)]} + 3HN(SiMe_3)_2 + 2i\text{-butane} \quad (1)$$

$$Sm[N(SiMe_3)_2]_3 + Al(i\text{-}Bu)_3 \xrightarrow[\text{THF}]{6t\text{-Bu-OH}} \underset{\mathbf{2}}{[(THF)_2Sm(O\text{-}t\text{-}Bu)_4Al(O\text{-}t\text{-}Bu)(i\text{-}Bu)_2]} + 3HN(SiMe_3)_2 + i\text{-butane} \quad (2)$$

Table 1. Selected Bond Distances (Å) and Angles (deg) for $\{[(i\text{-}Pr\text{-}O)(i\text{-}Bu)Al(\mu\text{-}O\text{-}i\text{-}Pr)_2Sm(O\text{-}i\text{-}Pr)(HO\text{-}i\text{-}Pr)](\mu\text{-}O\text{-}i\text{-}Pr)\}_2$ (**1**)

Sm1−O1	2.323(4)	Al1−O4	1.775(4)
Sm1−O1*	2.316(4)	Al1−O5	1.792(4)
Sm1−O2	2.491(4)	Al1−O6	1.749(5)
Sm1−O3	2.101(4)	Al1−C19	1.890(7)
Sm1−O4	2.429(4)	Sm1−O5	2.446(4)
O2−O6	2.693(6)		
O1−Sm1−O2	90.18(13)	O1*−Sm1−O1	71.88(15)
O1−Sm1−O3	105.36(15)	O1*−Sm1−O2	157.52(14)
O1−Sm1−O4	94.71(13)	O1*−Sm1−O3	106.27(16)
O1−Sm1−O5	155.78(13)	O1*−Sm1−O4	90.69(13)
O2−Sm1−O3	91.22(16)	O1*−Sm1−O5	112.89(13)
O2−Sm1−O4	77.07(14)	O4−Al1−O5	89.75(18)
O2−Sm1−O5	78.19(13)	O4−Al1−O6	106.7(2)
O3−Sm1−O4	156.86(15)	O5−Al1−O6	105.7(2)
O3−Sm1−O5	96.16(15)	O4−Al1−C19	117.8(3)
O4−Sm1−O5	62.17(12)	O5−Al1−C19	119.7(3)
C1−O1−Sm1	125.9(4)	O6−Al1−C19	114.0(3)
C1−O1−Sm1*	125.9(4)	Sm1*−O1−Sm1	108.12(15)
C4−O2−Sm1	128.4(4)	Al1−O4−Sm1	102.08(17)
C7−O3−Sm1	178.5(6)	Al1−O5−Sm1	100.95(16)
C13−O5−Sm1	123.6(4)	C10−O4−Al1	132.3(4)
C10−O4−Sm1	123.2(3)	C13−O5−Al1	126.6(4)
C16−O6−Al1	127.5(4)	C20−C19−Al1	125.0(5)

A notable feature of both products is the presence of aluminum-bound *iso*-butyl groups, despite the addition of sufficient alcohol to protonate all Al−C bonds. In complex **1**, we even observe a coordinated alcohol ligand in the same molecule as an aluminum-bound *iso*-butyl group. We note that there have been a few previous reports of this surprising resilience of an Al−C bond to protonolysis.[26−28] The low yields of **1** and **2** are due in part to the high solubility of these complexes even in nonpolar solvents such as pentane and bis(trimethylsilyl)ether. Solution ^1H NMR spectra of **1** and **2** reveal only one type of alkoxide ligand resonance in each case, indicating the presence of fluxional processes which rapidly exchange bridge and terminal ligands on the NMR time scale.

Crystals of **1** suitable for an X-ray diffraction study were grown by cooling a concentrated pentane solution to −35 °C; selected bond lengths and angles are presented in Table 1. Complete details of the structural analyses of compounds **1**−**5** are listed in Table 6. An ORTEP drawing giving the atom-numbering scheme used in the tables is shown in Figure 1. The overall molecular geometry of **1** comprises a

(12) Rao, R. P. *J. Electrochem. Soc.* **1996**, *143*, 189.
(13) Erickson, D. D.; Wood, W. P. *Ceram. Trans.* **1994**, *46*, 463.
(14) Masuda, K.; Sano, T.; Mizukami, F.; Miyazaki, M. *Catal. Lett.* **1995**, *32*, 139.
(15) He, Q.; Najafi, S. I.; Honkanen, S. *Proc. SPIE-Int. Soc. Opt. Eng.* **1993**, *1794*, 309.
(16) He, Q.; Lafreniere, S.; Najafi, S. I.; Honkanen, S. *S. Proc. SPIE-Int. Soc. Opt. Eng.* **1993**, *1794*, 303.
(17) Edelmann, A.; Gilje, J. W.; Edelmann, F. T. *Polyhedron* **1992**, *11*, 2421.
(18) Mehrotra, R. C.; Agrawal, M. M.; Tripathi, U. D.; Bindal, S. R. *Proc. Rare Earth Res. Conf., 7th* **1969**, *2*, 759.
(19) Wijk, M.; Norrestam, R.; Nygren, M.; Westin, G. *Inorg. Chem.* **1996**, *35*, 1077.
(20) Tripathi, U. M.; Singh, A.; Mehrotra, R. C.; Goel, S. C.; Chiang, M. Y.; Buhro, W. E. *Chem. Commun.* **1992**, 152.
(21) Evans, W. J.; Boyle, T. J.; Ziller, J. W. *J. Am. Chem. Soc.* **1993**, *115*, 5084.
(22) Biagini, P.; Lugli, G.; Abis, L.; Millini, R. *J. Organomet. Chem.* **1994**, C16.
(23) Gordon, J. C.; Giesbrecht, G. R.; Brady, J. T.; Clark, D. L.; Keogh, D. W.; Scott, B. L.; Watkin, J. G. *Organometallics* **2002**, *21*, 127.
(24) Giesbrecht, G. R.; Gordon, J. C.; Brady, J. T.; Clark, D. L.; Keogh, D. W.; Michalczyk, R.; Scott, B. L.; Watkin, J. G. *Eur. J. Inorg. Chem.* **2002**, 723.
(25) Tripathi, U. M.; Singh, A.; Mehrotra, R. C. *Polyhedron* **1993**, *12*, 1947.
(26) Mason, M. R.; Smith, J. M.; Bott, S. G.; Barron, A. R. *J. Am. Chem. Soc.* **1993**, *115*, 4971.
(27) Harlan, C. J.; Mason, M. R.; Barron, A. R. *Organometallics* **1994**, *13*, 2957.
(28) McMahon, C. N.; Bott, S. G.; Barron, A. R. *Dalton Trans.* **1997**, 3129.

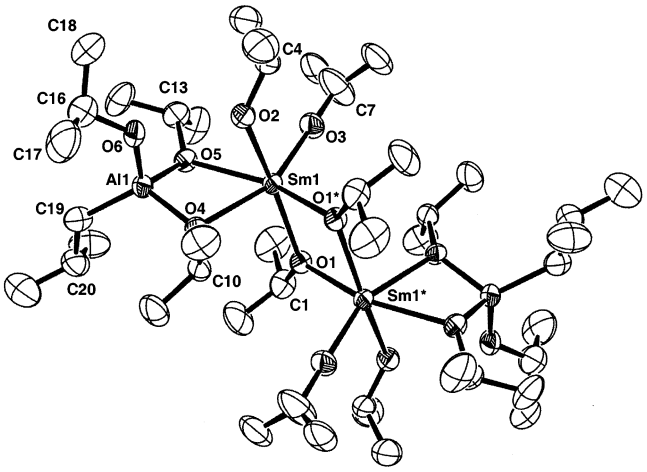

Figure 1. ORTEP view of {[(*i*-Pr-O)(*i*-Bu)Al(μ-O-*i*-Pr)$_2$Sm(O-*i*-Pr)(HO-*i*-Pr)](μ-O-*i*-Pr)}$_2$ (**1**) drawn with 30% probability ellipsoids. The asterisk designation (*) refers to atoms connected by a symmetry operation.

tetranuclear complex which may be viewed as two Al(O-*i*-Pr)$_2$(*i*-Bu) units capping either end of a centrosymmetric Sm$_2$-(O-*i*-Pr)$_6$(HO-*i*-Pr)$_2$ core. The geometry about the samarium metal centers is highly distorted octahedral, with the ligands involved in bridging deviating most widely from expected octahedral values (O1−Sm1−O1* = 71.88(15)° and O4−Sm1−O5 = 62.17(12)°). Similarly, the demands of the bridging ligands distort the geometry about the aluminum away from ideal tetrahedral (e.g., O4−Al1−O5 = 89.75(18)°). The short Sm1−O3 distance of 2.101(4) Å and obtuse Sm1−O3−C7 angle of 178.5(6)° allow this ligand to be definitively identified as a terminal *iso*-propoxide, while the very long Sm1−O2 distance of 2.491(4) Å and acute Sm1−O2−C4 angle of 128.4(4)° strongly suggest this to be a *iso*-propyl alcohol ligand. A close study of the structure also indicates that the OH proton of this alcohol ligand is involved in hydrogen-bonding with the oxygen atom (O6) of the aluminum-bound terminal *iso*-propoxide ligand. Two pieces of evidence may be proposed to support this hypothesis: (i) the *iso*-propyl group of this ligand (comprising C16, C17, and C18) is oriented directly away from the *iso*-propyl alcohol ligand, producing an ideal cavity between O2 and O6 for a bridging hydrogen (note that the O2−O6 distance of 2.693(6) Å lies within the expected range for fragments that are known to contain O−H···O bonding interactions[29]), and (ii) the Al1−O6 distance of 1.749(5) Å lies at the upper end of the range normally observed for Al−O bonds in terminal aluminum alkoxides,[30−33] which suggests an Al−O bond slightly weakened by participation in a Sm−O−H···O−Al bridge. By comparison, Al−O(H) distances within neutral trivalent aluminum complexes typically lie within the range 1.81−1.90 Å.[34−38] Bridging Sm−O distances lie in the range 2.316(4)−2.446(4) Å and are typical of those previously reported for μ_2-samarium alkoxide ligands.[39,40] While this work was in progress, we became aware of a crystal structure determination of a closely related erbium analogue of **1**, namely {[(*i*-Pr-O)$_2$Al(μ-O-*i*-Pr)$_2$Er(O-*i*-Pr)-(HO-*i*-Pr)](μ-O-*i*-Pr)}$_2$.[41] The erbium compound was found to crystallize in the same space group as **1** and is essentially isostructural with the exception that **3** has two terminal *iso*-propoxide ligands on aluminum, in contrast to the *iso*-propoxide and *iso*-butyl ligands in **1**. Bond lengths and angles within **1** are all comparable to those in the erbium analogue, with the exception that Sm−O bond lengths are 0.07−0.09 Å longer than the corresponding Er−O distances, which is in agreement with the difference in ionic radii (Sm^{3+} = 0.958 Å, Er^{3+} = 0.89 Å).[42] The erbium complex features terminal Al−O bond lengths of 1.740(2) Å (hydrogen-bonded) and 1.697(2) Å, compared with an Al−O distance of 1.749(5) Å and an Al−C distance of 1.890(7) Å in **1**. Further evidence for the presence of an *iso*-butyl, rather than an *iso*-propoxide, ligand bound to aluminum in **1** includes the following: (i) attempts to model the CH_2 group of the *iso*-butyl ligand as an oxygen led to significantly larger temperature factors which were not consistent with those seen for other *iso*-propoxide ligands within the molecule; (ii) the Al−C distance of 1.890(7) Å is significantly longer than that expected for a terminal Al−O alkoxide bond (typically 1.68−1.72 Å);[30−33] (iii) elemental analysis results are in much closer agreement with the formula containing an *iso*-butyl, rather than an *iso*-propoxide, ligand; (iv) ^{1}H NMR spectra show resonances consistent with the presence of an *iso*-butyl ligand, in particular, the upfield-shifted Al−CH_2 resonance at δ −1.20. We note, however, that the Al−C bond distance of 1.890(7) Å lies at the short end of the range of Al−CH_2 bond lengths found in the literature (typically 1.92−2.02 Å)[43−49] and postulate that a small quantity of the compound bearing two

(29) Steiner, T. *Angew. Chem., Int. Ed.* **2002**, *41*, 48 and references therein.
(30) Garbauskas, M. F.; Wengrovius, J. H.; Going, R. C.; Kasper, J. S. *Acta Crystallogr., Sect. C* **1984**, *40*, 1536.
(31) Noth, H.; Schlegel, A.; Knizek, J.; Schwenk, H. *Angew. Chem., Int. Ed. Engl.* **1997**, *36*, 2640.
(32) Chisholm, M. H.; DiStasi, V. F.; Streib, W. E. *Polyhedron* **1990**, *9*, 253.
(33) Folting, K.; Streib, W. E.; Caulton, K. G.; Poncelet, O.; Hubert-Pfalzgraf, L. G. *Polyhedron* **1991**, *10*, 1639.
(34) McMahon, C. N.; Bott, S. G.; Barron, A. R. *J. Chem. Soc., Dalton Trans.* **1997**, 3129.
(35) McMahon, C. N.; Alemany, L.; Callendar, R. L.; Bott, S. G.; Barron, A. R. *Chem. Mater.* **1999**, *11*, 3181.
(36) McMahon, C. N.; Obrey, S. J.; Keys, A.; Bott, S. G.; Barron, A. R. *J. Chem. Soc., Dalton Trans.* **2000**, 2151.
(37) DiMarco, V. B.; Bombi, G. G.; Tapparo, A.; Powell, A. K.; Anson, C. E. *J. Chem. Soc., Dalton Trans.* **1999**, 2427.
(38) Belanger-Gariepy, F.; Hoogsteen, K.; Sharma, V.; Wuest, J. D. *Inorg. Chem.* **1991**, *30*, 4140.
(39) Steudel, R.; Stehr, J.; Siebel, E.; Fischer, R. D. *J. Organomet. Chem.* **1996**, *510*, 197.
(40) Hou, Z. M.; Fujita, A.; Yamakazi, H.; Wakatsuki, Y. *J. Am. Chem. Soc.* **1996**, *118*, 7843.
(41) Kritikos, M.; Wijk, M.; Westin, G. *Acta Crystallogr., Sect. C* **1998**, *54*, 576.
(42) Shannon, R. D.; Prewitt, C. T. *Acta Crystallogr.* **1970**, *26*, 1046.
(43) Rutherford, D.; Atwood, D. A. *J. Am. Chem. Soc.* **1996**, *118*, 11535.
(44) Hendershot, D. G.; Barber, M.; Kumar, R.; Oliver, J. P. *Organometallics* **1991**, *10*, 3302.
(45) Schauer, S. J.; Pennington, W. T.; Robinson, G. H. *Organometallics* **1992**, *11*, 3287.
(46) Schonberg, P. R.; Paine, R. T.; Campana, C. F.; Duesler, E. N. *Organometallics* **1982**, *1*, 799.
(47) Rahman, A. F. M.; Siddiqui, K. F.; Oliver, J. P. *Organometallics* **1982**, *1*, 881.
(48) van Vliet, M. R. P.; Buysingh, P.; van Koten, G.; Vrieze, K.; Kojic-Prodic, B.; Spek, A. L. *Organometallics* **1985**, *4*, 1701.
(49) Hartner, F. M.; Clift, S. M.; Schwartz, J.; Tulip, T. H. *Organometallics* **1987**, *6*, 1346.

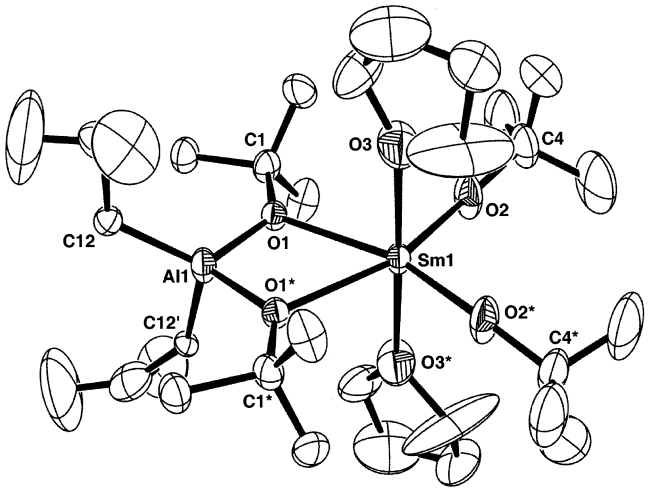

Figure 2. ORTEP view of $[(THF)_2Sm(O\text{-}t\text{-}Bu)_2(\mu\text{-}O\text{-}t\text{-}Bu)_2Al(i\text{-}Bu)_2]$ (**2**) drawn with 30% probability ellipsoids. The second orientation of the disordered *iso*-butyl group is not shown for clarity. The asterisk designation (*) refers to atoms connected by a symmetry operation; the prime designation (′) refers to one of two orientations possible because of disorder.

Table 2. Selected Bond Distances (Å) and Angles (deg) for $[(THF)_2Sm(O\text{-}t\text{-}Bu)_2(\mu\text{-}O\text{-}t\text{-}Bu)_2Al(i\text{-}Bu)_2]$ (**2**)

Sm1−O1	2.488(6)	Al1−O1	1.771(6)
Sm1−O2	2.109(7)	Al1−C12	1.882(14)
Sm1−O3	2.470(10)	Al1−C12′	1.873(18)
O1−Sm1−O2	98.4(3)	O1−Sm1−O3	89.49(19)
O2−Sm1−O3	90.38(14)	O2−Sm1−O2*	101.3(5)
O3−Sm1−O3*	178.8(4)	O2−Sm1−O1*	160.3(3)
O2*−Sm1−O1	160.3(3)	O1−Sm1−O1*	61.9(3)
O1−Al1−O1*	92.4(4)	O1−Al1−C12′	127.9(3)
C12−Al1−C12′	112.0(7)	O1−Al1−C12	98.7(3)
C1−O1−Al1	131.1(6)	Al1−O1−Sm1	102.9(3)
C1−O1−Sm1	126.0(5)	C4−O2−Sm1	160.0(8)

iso-propoxide ligands on aluminum may be cocrystallized with **1**, resulting in an apparently shortened Al−C bond.

Single crystals of **2** were grown from a concentrated hexane solution at −35 °C. An ORTEP representation of compound **2** is available in Figure 2; selected bond lengths and angles are presented in Table 2. Compound **2** crystallizes in the orthorhombic space group *Cmcm* with no unusual intermolecular contacts. The overall molecular geometry comprises a pseudo-octahedral samarium metal center bearing two terminal *tert*-butoxide and two THF ligands, which bridges to an aluminum metal center by means of two μ_2-*tert*-butoxide ligands. The aluminum bears two *iso*-butyl ligands to complete its distorted tetrahedral coordination sphere. The overall geometry is thus very similar to that previously observed in the mixed-metal yttrium−aluminum alkoxide complex $(t\text{-Bu-O})Cl(THF)_2Y(\mu\text{-O-}t\text{-Bu})_2AlMe_2$.[21] Disorder was observed within the *iso*-butyl, THF, and terminal *tert*-butoxide ligands and was modeled using partial occupancy carbon and oxygen atoms. Bond angles about the samarium are reasonably close to octahedral values, with the exception of the angle between the bridging ligands (O1−Sm1−O1*), which is reduced to 61.9(3)°. Similarly, the angles about aluminum are distorted from tetrahedral, with the O1−Al1−O1* angle being reduced to 92.4(4)° while the C12−Al1−C12′ angle is 112.0(7)°. The Sm−O distance to the terminal *tert*-butoxide ligands (Sm1−O2 = 2.109(7) Å) is directly comparable to the value observed for the terminal alkoxide in **1**, while the Sm−O(THF) distance of 2.470(10) Å is typical of those found in other THF adducts of samarium(III).[50−52] The Al−C distances of 1.873(18) and 1.882(14) Å for the two disordered *iso*-butyl groups are very similar to that of 1.890(7) Å found in **1** and, once again, are slightly shorter than those previously observed for Al−Me and Al−*i*-Bu linkages. Upon prolonged exposure to inert atmosphere, crystals of **2** were seen to powder presumably because of loss of coordinated THF. Elemental analyses of these samples were in close agreement with a THF-free formulation.

In contrast to the syntheses of **1** and **2**, reaction of an equimolar mixture of $Ln[N(SiMe_3)_2]_3$ (Ln = Nd, Sm) and $Al(i\text{-Bu})_3$ with the bulkier aryloxide, HO-2,4,6-$Me_3C_6H_2$, instead yielded the Lewis base adducts $Sm(OAr)_3(THF)_3$ (**3**) and $[Nd(\mu\text{-OAr})(OAr)_2(py)_2]_2$ (**4**) (eqs 3 and 4).

$$Sm[N(SiMe_3)_2]_3 + Al(i\text{-Bu})_3 \xrightarrow[THF]{6ArOH} \underset{\mathbf{3}}{Sm(OAr)_3(THF)_3} + 3HN(SiMe_3)_2 + \text{“}Al(OAr)_3 + 3i\text{-butane”} \quad (3)$$

(Ar = 2,4,6-$Me_3C_6H_2$)

$$Nd[N(SiMe_3)_2]_3 + Al(i\text{-Bu})_3 \xrightarrow[pyridine]{6ArOH} \underset{\mathbf{4}}{[Nd(\mu\text{-OAr})(OAr)_2(py)_2]_2} + 3HN(SiMe_3)_2 + \text{“}Al(OAr)_3 + 3i\text{-butane”} \quad (4)$$

It was uncertain whether alcoholysis of the trialkylaluminum reagent occurred to produce $Al(OAr)_3$, or if the bulky nature of the aryloxide group disfavored the coordination and subsequent formation of mixed-metal species. The incomplete alcoholysis of $Al(i\text{-Bu})_3$ by *iso*-propyl alcohol and *tert*-butyl alcohol in the syntheses of **1** and **2** suggests that the formation of $Al(OAr)_3$ may require more forcing conditions than those employed here;[53] alternatively, the crystal structures of **3** and **4** imply that the formation of lanthanide−aluminum complexes with bridging O-2,4,6-$Me_3C_6H_2$ groups may not be feasible simply on the basis of sterics (see later).

Crystals of **3** that were suitable for X-ray diffraction were grown from a THF/hexane mixture at −10 °C. An ORTEP view of the structure is presented in Figure 3; selected bond lengths and angles are available in Table 3. The overall structure of **3** is similar to that of $Sm(O\text{-}2,6\text{-}i\text{-}Pr_2C_6H_3)_3(THF)_3$,[54] with the aryloxide ligands in a facial arrangement. The geometry about the samarium center is distorted octahedral, as evidenced by the O1−Sm1−O3 angle of 103.39(13)° and the O5−Sm1−O6 angle (77.46(11)°). The Sm−O(Ar) distances of 2.154(3), 2.163(4), and 2.162(4) Å

(50) Evans, W. J.; Drummond, D. K.; Hughes, L. A.; Zhang, H.; Atwood, J. L. *Polyhedron* **1988**, *7*, 1693.
(51) Evans, W. J.; Ulibarri, T. A.; Ziller, J. W. *Organometallics* **1991**, *10*, 134.
(52) Clark, D. L.; Gordon, J. C.; Huffman, J. C.; Watkin, J. G.; Zwick, B. D. *Polyhedron* **1996**, *15*, 2279.
(53) Athar, T.; Bohra, R.; Mehrotra, R. C. *Indian J. Chem.* **1989**, *28A*, 492.
(54) Xie, Z.; Chui, K.; Yang, Q.; Mak, T. C. W.; Sun, J. *Organometallics* **1998**, *17*, 3937.

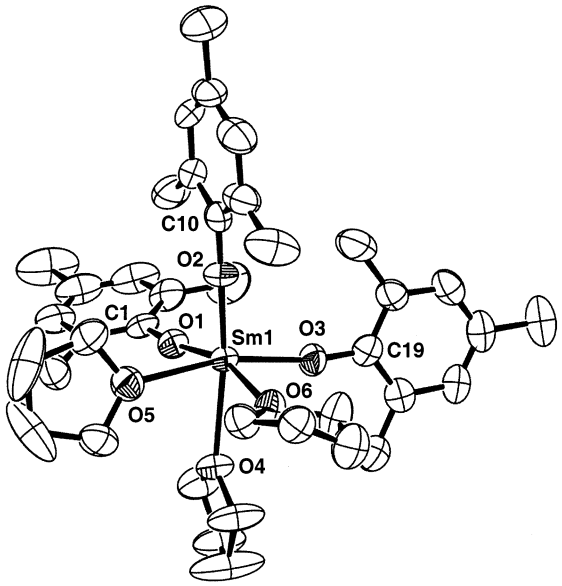

Figure 3. ORTEP view of $Sm(OAr)_3(THF)_3$ (Ar = 2,4,6-$Me_3C_6H_2$) (**3**) drawn with 30% probability ellipsoids.

Table 3. Selected Bond Distances (Å) and Angles (deg) for $Sm(OAr)_3(THF)_3$ (Ar = 2,4,6-$Me_3C_6H_2$) (**3**)

Sm1−O1	2.154(3)	Sm1−O2	2.163(4)
Sm1−O3	2.162(4)	Sm1−O4	2.568(4)
Sm1−O5	2.531(3)	Sm1−O6	2.526(3)
O1−Sm1−O2	102.57(14)	O1−Sm1−O3	103.39(13)
O1−Sm1−O4	84.36(13)	O1−Sm1−O5	89.34(13)
O1−Sm1−O6	161.49(13)	O2−Sm1−O3	102.39(14)
O2−Sm1−O4	162.75(13)	O2−Sm1−O5	85.83(13)
O2−Sm1−O6	89.51(13)	O3−Sm1−O4	91.12(13)
O3−Sm1−O5	162.73(12)	O3−Sm1−O6	87.34(12)
O4−Sm1−O5	78.40(12)	O4−Sm1−O6	80.35(12)
O5−Sm1−O6	77.46(11)	Sm1−O1−C1	171.4(4)
Sm1−O2−C10	168.6(4)	Sm1−O3−C19	170.0(3)

are similar to those in $Sm(O\text{-}2,6\text{-}i\text{-}Pr_2C_6H_3)_3(THF)_3$, indicating that the steric requirements of the O-2,6-*i*-$Pr_2C_6H_3$ and O-2,4,6-$Me_3C_6H_2$ ligands are comparable. The Sm−O−C(Ar) angles of 171.4(4)°, 168.6(4)°, and 170.0(3)° are also similar to those in $Sm(O\text{-}2,6\text{-}i\text{-}Pr_2C_6H_3)_3(THF)_3$ and fall into the range normally observed for $Ln(O\text{-}2,6\text{-}i\text{-}Pr_2C_6H_3)_3(THF)_x$ (x = 2, 3) compounds.[52,54−56] A similar structure has also been observed for $Y(O\text{-}2,6\text{-}Me_2C_6H_3)_3(THF)_3$.[57]

Crystals of **4** that were amenable to X-ray diffraction were grown by slow evaporation of a saturated toluene solution. An ORTEP view of the structure is presented in Figure 4; selected bond lengths and angles are available in Table 4. The addition of pyridine was necessary to confer crystallinity to the complex; as a result, each metal center is coordinated by two pyridine molecules. There is also one molecule of toluene per dimer in the lattice. The THF analogue of **4** has been crystallographically characterized, although bond lengths and angles were not reported.[58] As in $[Nd(\mu\text{-}OAr)(OAr)_2(THF)_2]_2$, each neodymium center in **4** is severely distorted from octahedral, being ligated by two terminal aryloxide groups, two bridging aryloxide ligands, and two terminal pyridine molecules. As is typical, the bridging Nd−O distances (Nd1−O1 = 2.424(2) Å, Nd1−O1* = 2.421(2) Å) are ∼0.2 Å longer than the terminal Nd−O distances (Nd1−O2 = 2.211(2) Å, Nd1−O3 = 2.220(2) Å). A similar variation in bond lengths was observed in the related complex $[Y(\mu\text{-}O\text{-}2,6\text{-}Me_2C_6H_3)(O\text{-}2,6\text{-}Me_2C_6H_3)_2(THF)]_2$.[57] The Nd−O−C(Ar) angles of the terminal aryloxide groups (Nd1−O1−C1 = 169.9(2)°, Nd1−O3−C19 = 164.9(2)°) are similar to those found in $[Y(\mu\text{-}O\text{-}2,6\text{-}Me_2C_6H_3)(O\text{-}2,6\text{-}Me_2C_6H_3)_2(THF)]_2$ as well as **3**; other bond lengths and angles are unremarkable.

We were also interested in the potential of generating mixed-metal alkoxides by utilizing reagents with the required groups already present in the precursors. Thus, we postulated that the reaction of $[Sm(OAr)_3]_2$ (Ar = 2,6-*i*-$Pr_2C_6H_3$) with $Al_2(O\text{-}t\text{-}Bu)_6$ may generate a mixed-metal species directly without the need for the synthesis of the necessary starting materials in situ. In this case, the isolated product was not $(ArO)_xSm[(\mu\text{-}OAr)(\mu\text{-}O\text{-}t\text{-}Bu)]_{3-x}Al(O\text{-}t\text{-}Bu)_x$ (x = 1, 2) as

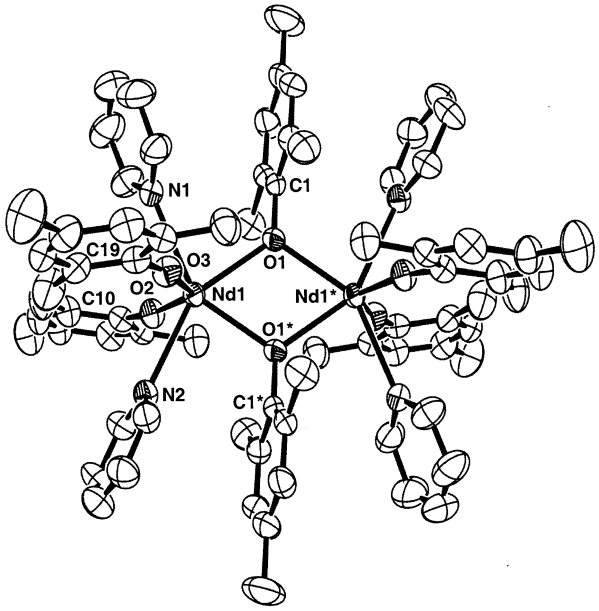

Figure 4. ORTEP view of $[Nd(\mu\text{-}OAr)(OAr)_2(py)_2]_2$ (Ar = 2,4,6-$Me_3C_6H_2$) (**4**) drawn with 30% probability ellipsoids. Interstitial toluene molecule omitted for clarity. The asterisk designation (*) refers to atoms connected by a symmetry operation.

Table 4. Selected Bond Distances (Å) and Angles (deg) for $[Nd(\mu\text{-}OAr)(OAr)_2(py)_2]_2$(toluene) (Ar = 2,4,6-$Me_3C_6H_2$) (**4**)

Nd1−O1	2.424(2)	Nd1−O1*	2.421(2)
Nd1−O2	2.211(2)	Nd1−O3	2.220(2)
Nd1−N1	2.648(3)	Nd1−N2	2.671(3)
O1−Nd1−O1*	66.51(9)	O1−Nd1−O2	110.09(9)
O1−Nd1−O3	106.78(9)	O1−Nd1−N1	80.33(9)
O1−Nd1−N2	150.41(9)	O1*−Nd1−O2	114.53(7)
O1*−Nd1−O3	109.17(9)	O1*−Nd1−N1	146.82(8)
O1*−Nd1−N2	83.96(8)	O2−Nd1−O3	133.81(9)
O2−Nd1−N1	80.75(10)	O2−Nd1−N2	79.65(9)
O3−Nd1−N1	80.52(10)	O3−Nd1−N2	80.35(9)
N1−Nd1−N2	129.22(9)	Nd1−O1−C1	126.54(19)
Nd1*−O1−C1	119.37(19)	Nd1−O2−C10	169.9(2)
Nd1−O3−C19	164.9(2)		

(55) Butcher, R. J.; Clark, D. L.; Grumbine, S. K.; Vincent-Hollis, R. L.; Scott, B. L.; Watkin, J. G. *Inorg. Chem.* **1995**, *34*, 5468.
(56) Barnhart, D. M.; Clark, D. L.; Gordon, J. C.; Huffman, J. C.; Vincent, R. L.; Watkin, J. G.; Zwick, B. D. *Inorg. Chem.* **1994**, *33*, 3487.
(57) Evans, W. J.; Olofson, J. M.; Ziller, J. W. *Inorg. Chem.* **1989**, *28*, 4308.
(58) Evans, W. J.; Ansari, M. A.; Khan, S. I. *Organometallics* **1995**, *14*, 558.

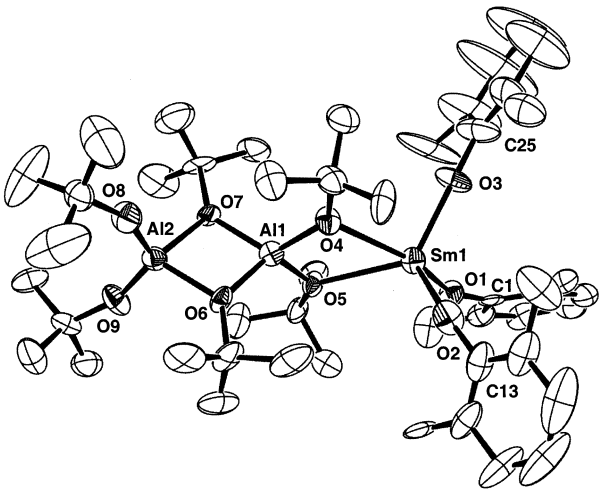

Figure 5. ORTEP view of $(ArO)_3Sm[(\mu\text{-O-}t\text{-Bu})_2Al_2(O\text{-}t\text{-Bu})_4]$ (Ar = 2,6-*i*-$Pr_2C_6H_3$) (**5**) drawn with 30% probability ellipsoids. Isopropyl methyl groups have been omitted for clarity.

Table 5. Selected Bond Distances (Å) and Angles (deg) for $(ArO)_3Sm[(\mu\text{-O-}t\text{-Bu})_2Al_2(O\text{-}t\text{-Bu})_4]$ (Ar = 2,6-*i*-$Pr_2C_6H_3$) (**5**)

Sm1−O1	2.184(6)	Sm1−O2	2.150(9)
Sm1−O3	2.130(7)	Sm1−O4	2.583(6)
Sm1−O5	2.572(6)	Al1−O4	1.729(6)
Al1−O5	1.734(6)	Al1−O6	1.817(7)
Al−O7	1.781(7)	Al2−O6	1.842(7)
Al2−O7	1.861(7)	Al2−O8	1.661(7)
Al2−O9	1.659(7)	O1−Sm1−O2	101.0(3)
O1−Sm1−O3	103.4(3)	O1−Sm1−O4	155.1(2)
O1−Sm1−O5	97.3(2)	O2−Sm1−O3	107.0(3)
O2−Sm1−O4	96.8(3)	O2−Sm1−O5	113.2(3)
O3−Sm1−O4	87.7(2)	O3−Sm1−O5	129.7(3)
O4−Sm1−O5	59.36(18)	Sm1−O1−C1	154.2(6)
Sm1−O2−C13	160.1(8)	Sm1−O3−C25	158.5(8)

expected, but the aluminum adduct, $(ArO)_3Sm[(\mu\text{-O-}t\text{-Bu})_2Al_2(O\text{-}t\text{-Bu})_4]$ (**5**) (eq 5).

$$[Sm(OAr)_3]_2 + 2Al_2(O\text{-}t\text{-Bu})_6 \xrightarrow{\text{toluene}} 2(ArO)_3Sm[(\mu\text{-O-}t\text{-Bu})_2Al_2(O\text{-}t\text{-Bu})_4] \quad (5)$$

(Ar = 2,6-*i*-$Pr_2C_6H_3$)

5

The solution ^{1}H NMR spectrum of the solid from the reaction mixture exhibited peaks due to only the starting materials; that is, a spectrum consistent with the structure of **5** was not observed. However, IR spectroscopy of the bulk sample indicated that the samarium dimer, $[Sm(OAr)_3]_2$, had been consumed in the reaction. Similarly, X-ray crystallography indicated the presence of an aluminum adduct of $[Sm(OAr)_3]_2$. Slow evaporation of a saturated toluene solution resulted in pale yellow crystals of **5**. An ORTEP drawing is shown in Figure 5; relevant bond lengths and angles are presented in Table 5. The solid-state structure of **5** can be viewed as a $Sm(OAr)_3$ unit coordinated via two bridging *tert*-butoxide groups to an intact $Al_2(O\text{-}t\text{-Bu})_6$ moiety. In this sense, the $Al_2(O\text{-}t\text{-Bu})_6$ group acts as a bidentate Lewis base to generate a five-coordinate samarium center, in much the same manner as $Sm(O\text{-}2,6\text{-}i\text{-}Pr_2C_6H_3)_3(THF)_2$.[52] The samarium center can be described as square pyramidal, with two terminal aryloxide ligands and two bridging *tert*-butoxide ligands in the base, and an aryloxide ligand (O3) occupying the apical position. The Sm−O−C(Ar) angles range from 154.2(6)° to 160.1(8)°, suggesting that the samarium center in compound **5** is comparable in terms of electrophilicity to the samarium center in **3**. This observation, coupled with the Sm−O(Ar) bond lengths of 2.184(6), 2.150(9), and 2.130(7) Å, supports our view of the $Al_2(O\text{-}t\text{-Bu})_6$ unit as a very weak Lewis base. The distances to the bridging *tert*-butoxide groups are significantly lengthened (Sm1−O4 = 2.583(6) Å, Sm1−O5 = 2.572(6) Å), presumably because of a weak interaction between the $Sm(OAr)_3$ and $Al_2(O\text{-}t\text{-Bu})_6$ groups[59] (supported by the inability to observe complex **5** by ^{1}H NMR spectroscopy), or a reflection of the sterics of the *tert*-butoxide units. Nonetheless, the X-ray crystal structure of **5** indicates that lanthanide−aluminum mixed-metal species utilizing simultaneous bridging *tert*-butoxide and aryloxide ligands are probably not feasible.

Conclusions

Alcoholysis of an equimolar mixture of a trialkylaluminum reagent and a samarium tris(amido) complex can produce mixed-metal alkoxide complexes which maintain the 1:1 metal stoichiometry. However, the aluminum-bound *iso*-butyl groups proved to be somewhat resistant to complete alcoholysis and were found to occupy terminal positions within the products. Attempts to generate products containing bulkier aryloxide ligands met with limited success, presumably as a result of the steric constraints imposed by the phenoxide ligands in the latter classes of compounds. We are currently pursuing further synthetic studies in this area in order to gain a more detailed understanding of the interplay between the sterics of alkoxide/aryloxide ligation, ionic radius of the lanthanide ion in question, and the solid-state structures that result.

Experimental Section

General Considerations. All manipulations were carried out under an inert atmosphere of oxygen-free UHP grade argon using standard Schlenk techniques or under oxygen-free helium in an Innovative Technologies glovebox or a Vacuum Atmospheres glovebox. HO-2,4,6-$Me_3C_6H_2$ was purchased from Aldrich and used as received. Al(*i*-Bu)$_3$ was purchased as a 1.0 M toluene solution from Aldrich and used as received. $Al_2(O\text{-}t\text{-Bu})_6$ was purchased from Aldrich and recrystallized from toluene prior to use. Pyridine was purchased from Aldrich and distilled over sodium prior to use. $Sm[N(SiMe_3)_2]_3$,[60] $Nd[N(SiMe_3)_2]_2$,[60] and $[Sm(OAr)_3]_2$ (Ar = 2,6-*i*-$Pr_2C_6H_3$)[56] were prepared according to literature procedures. *iso*-Propyl alcohol and *tert*-butyl alcohol were distilled from sodium under inert atmosphere. Toluene, THF, diethyl ether, pentane, and hexanes were deoxygenated by passage through a column of supported copper redox catalyst (Cu-0226 S) and dried by passing through a second column of activated alumina. C_6D_6 was degassed, dried over Na−K alloy, and trap-to-trap distilled before use. ^{1}H NMR spectra were recorded on a Varian Unity 300 spectrometer or a Bruker AM-400 spectrometer at ambient temperature; chemical

(59) Cayton, R. H.; Chisholm, M. H.; Davidson, E. R.; DiStasi, V. F.; Du, P.; Huffman, J. C. *Inorg. Chem.* **1991**, *30*, 1020.
(60) Evans, W. J.; Golden, R. E.; Ziller, J. W. *Inorg. Chem.* **1991**, *30*, 4963.

shifts are given relative to residual C_6D_5H (7.15 ppm). Infrared spectra were recorded on a Digilab FTS-40 FT-IR spectrometer; solid-state spectra were taken as Nujol mulls between KBr plates. Elemental analyses were performed on a Perkin-Elmer 2400 CHN analyzer. Elemental analysis samples were prepared and sealed in tin capsules in the glovebox prior to combustion.

{[(*i*-Pr−O)(*i*-Bu)Al(*μ*-O-*i*-Pr)$_2$Sm(O-*i*-Pr)(HO-*i*-Pr)](*μ*-O-*i*-Pr)}$_2$ (1). To a stirred solution of Sm[N(SiMe$_3$)$_2$]$_3$ (0.500 g, 0.80 mmol) and Al(*i*-Bu)$_3$ (0.80 mL of a 1.0 M toluene solution, 0.80 mmol) in toluene (5 mL) was added *iso*-propyl alcohol (0.36 mL, 4.8 mmol) at room temperature. After 2 days of stirring, all solvent was removed under vacuum to leave a viscous oil. This was dissolved in pentane (5 mL) and the volume reduced to 2 mL, at which point the solution was placed in the −35 °C drybox freezer. Over several days, a small number of colorless crystals were deposited (200 mg, 21% yield). ^{1}H NMR (300 MHz, C_6D_6): *δ* 2.50 (br, OCH*Me*$_2$), 2.29 (m, OC*H*Me$_2$), 1.68 (m, CH$_2$C*H*Me$_2$), 0.78 (d, $^3J_{H-H}$ = 6 Hz, CH$_2$CH*Me*$_2$), −1.20 (br m, AlC*H*$_2$). IR (Nujol, cm^{-1}): 3100 (br w), 1462 (s), 1377 (s), 1366 (sh s), 1334 (w), 1161 (s), 1130 (s), 1069 (w), 1036 (w), 999 (s), 965 (s), 833 (m), 678 (m), 656 (m). Anal. Calcd for $C_{44}H_{104}Al_2O_{12}Sm_2$: C, 44.78; H, 8.88. Found: C, 44.76; H, 8.74.

[(THF)$_2$Sm(O-*t*-Bu)$_2$(*μ*-O-*t*-Bu)$_2$Al(*i*-Bu)$_2$] (2). To a stirred solution of Sm[N(SiMe$_3$)$_2$]$_3$ (0.500 g, 0.80 mmol) and Al(*i*-Bu)$_3$ (0.80 mL of a 1.0 M toluene solution, 0.80 mmol) in toluene (5 mL) was added *tert*-butyl alcohol (0.45 mL, 4.8 mmol) at room temperature. After stirring for 12 h, all solvent was removed under vacuum to leave a viscous oil. This was redissolved in hexanes (5 mL) and the volume reduced to 2 mL, at which point 0.2 mL of THF was added. The solution was then placed in a −35 °C freezer. Over several days, a small number of colorless crystals were deposited (100 mg, 17% yield). ^{1}H NMR (300 MHz, C_6D_6): *δ* 2.29 (br s, *t*-Bu), 0.78 (br, CH$_2$CH*Me*$_2$), −0.15 (v br, α-THF), −0.54 (br, *β*-THF), C*H*$_2$CHMe$_2$ obscured by THF. IR (Nujol, cm^{-1}): 1462 (s), 1380 (s), 1358 (s), 1308 (w), 1223 (s), 1187 (s), 1034 (s), 999 (s), 978 (s), 933 (s), 883 (sh m), 818 (w), 771 (s), 661 (s), 620 (m). Anal. Calcd for $C_{32}H_{70}AlO_6Sm$: C, 52.78; H, 9.69. Calcd for $C_{24}H_{54}AlO_4Sm$ [**2** − 2THF]: C, 49.35; H, 9.32. Found: C, 49.65; H, 8.90.

Sm(OAr)$_3$(THF)$_3$ (Ar = 2,4,6-Me$_3$C$_6$H$_2$) (3). Sm[N(SiMe$_3$)$_2$]$_3$ (500 mg, 0.80 mmol) was dissolved in 50 mL of hexanes, forming a colorless solution. Al(*i*-Bu)$_3$ (0.80 mL of a 1.0 M toluene solution, 0.80 mmol) was added followed by an ethereal solution (5 mL) of HO-2,4,6-Me$_3$C$_6$H$_2$ (650 mg, 4.8 mmol), forming an instantaneous blue precipitate. The reaction mixture was then filtered to yield a yellow-green solution. The solution was left to evaporate, producing a viscous oil. This was redissolved in approximately 5 mL of hexanes, and pyridine (0.5 mL) was added. After stirring for 5 min, the solvent was removed under vacuum, yielding a slightly oily solid. Hexanes (10 mL) were added, and the resulting pale solid was collected by filtration, washed with hexanes (5 mL), and dried to yield a slightly yellow solid (180 mg, 28% yield). A portion of this solid (84 mg) was dissolved in a 1:1 mixture of hexanes/THF (approximately 2 mL). Cooling to −10 °C yielded pale yellow crystals of **3**. ^{1}H NMR (400 MHz, C_6D_6): *δ* 7.80 (br s, 6H, *m*-Ph), 3.80 (br s, 12H, THF), 2.90 (br s, 18H, *o*-C*H*$_3$Ph), 2.80 (br s, 9H, *p*-C*H*$_3$Ph), 2.10 (br s, 12H, THF). IR (Nujol, cm^{-1}): 1607 (m), 1465 (m), 1310 (s), 1277 (s), 1262 (m), 1160 (w), 1150 (w), 1025 (m), 955 (w), 915 (w), 860 (m), 830 (s), 821 (s), 742 (m), 722 (w). Anal. Calcd for $C_{39}H_{57}O_6Sm$: C, 60.66; H, 7.44. Found: C, 60.52; H, 7.47.

[Nd(*μ*-OAr)(OAr)$_2$(py)$_2$]$_2$ (Ar = 2,4,6-Me$_3$C$_6$H$_2$) (4). Nd[N(SiMe$_3$)$_2$]$_3$ (500 mg, 0.80 mmol) was dissolved in 50 mL of hexane, forming a colorless solution. Al(*i*-Bu)$_3$ (0.80 mL of a 1.0 M toluene solution, 0.80 mmol) was added followed by an ethereal solution (5 mL) of HO-2,4,6-Me$_3$C$_6$H$_2$ (650 mg, 4.8 mmol), forming a purple solid. After filtration of the solid, the solvent was removed in vacuo, yielding a slightly oily solid. Diethyl ether (50 mL) was added and the solution concentrated to 20 mL, at which point a pale solid began to precipitate from solution. Cooling to −10 °C failed to deposit crystalline material from solution. The solution was filtered again, pyridine (1 mL) was added, and the mixture stirred for several minutes. Removal of the solvent yielded an oily solid. Washing the solid with hexanes (3 × 5 mL) produced a pale blue solid (240 mg, 38% yield). A 100 mg portion of this material was taken up in toluene (5 mL) and the solution allowed to slowly evaporate in the glovebox atmosphere. Over a period of several days, large lavendar crystals were obtained. The paramagnetism of **4** did not allow for characterization by ^{1}H NMR spectroscopy. IR (Nujol, cm^{-1}): 1599(m), 1308 (m), 1254 (m), 1240 (m), 1217 (m), 1160 (w), 1146 (w), 1030 (w), 852 (w), 804 (m), 777 (w), 740 (w), 721 (m), 700 (w). Anal. Calcd for $C_{64}H_{76}N_2Nd_2O_6$ [**4** − 2(pyridine)]: C, 61.11; H, 6.09; N, 2.23. Found: C, 55.19; H, 6.09; N, 2.32. Independently prepared samples of **4** consistently analyzed low in carbon because of incomplete combustion.

(ArO)$_3$Sm[(*μ*-O-*t*-Bu)$_2$Al$_2$(O-*t*-Bu)$_4$] (Ar = 2,6-*i*-Pr$_2$C$_6$H$_3$) (5). [Sm(OAr)$_3$]$_2$ (1.0 g, 0.73 mmol) was dissolved in toluene (80 mL) producing a bright yellow solution. A toluene solution (15 mL) of Al$_2$(O-*t*-Bu)$_6$ (720 mg, 1.5 mmol) was added and stirred at room temperature for 1 h. The solvent was then removed under vacuum to yield a pale yellow solid (1.6 g, 93% yield). Slow evaporation of a yellow-green toluene solution yielded X-ray quality crystals of **5**. The ^{1}H NMR spectrum consisted of peaks corresponding to unreacted starting materials only. IR (Nujol, cm^{-1}): 1587 (m), 1397 (w), 1320 (m), 1255 (m), 1227 (m), 1200 (m), 1168 (w), 1071 (w), 1038 (w), 937 (m), 910 (w), 874 (m), 848 (w), 809 (w), 795 (m), 775 (w), 749 (m), 717 (m), 691 (w). Anal. Calcd for $C_{60}H_{105}Al_2O_9Sm$: C, 61.34; H, 9.01. Found: C, 61.10; H, 9.03.

Crystallographic Studies. Crystals of **1**−**5** were mounted on a thin glass fiber using a small dot of silicone grease. The crystal was then immediately placed on a Siemens P4/PC diffractometer (for **1** and **2**) or a Bruker P4/CCD/PC diffractometer (for **3**−**5**) and cooled to 203 K. The data were collected using a sealed, graphite monochromatized Mo Kα X-ray source. A hemisphere of data was collected using *ω* scans (for **1** and **2**) or a combination of *φ* and *ω* scans (**3**−**5**), with 30 s frame exposures and 0.3° frame widths. Data collection and initial indexing and cell refinement were handled using XSCANS software[61] (for **1** and **2**) or SMART software[62] (for **3**−**5**). For compounds **1** and **2**, all data reduction, including Lorentz and polarization corrections and structure solution and graphics, were performed using SHELXTL.[63] Frame integration and final cell parameter calculations for **3**−**5** were carried out using SAINT[64] software. The data were corrected for absorption using the ellipsoid option in the XEMP facility of SHELXTL or the SADABS[65] program. Decay of reflection intensity was not observed.

The structures were solved using direct methods and difference Fourier techniques. The initial solutions revealed all non-hydrogen

(61) *XSCANS* version 4.2/360; Siemens Analytical X-ray Instruments, Inc.: Madison, WI, 1993.
(62) *SMART* version 4.210; Bruker Analytical X-ray Systems, Inc.: Madison, WI, 1996.
(63) *SHELXTL* PC version 4.2/360; Siemens Analytical X-ray Instruments, Inc.: Madison, WI, 1993.
(64) *SAINT* version 4.05; Bruker Analytical X-ray Systems, Inc.: Madison, WI, 1996.
(65) Sheldrick, G. *SADABS*, first release; University of Gottingen: Gottingen, Germany, 1996.

Table 6. Crystallographic Data[a]

	1	**2**	**3**	**4**·(toluene)	**5**
formula	$C_{44}H_{102}Al_2O_{12}Sm_2$	$C_{32}H_{70}AlO_6Sm$	$C_{39}H_{57}O_6Sm$	$C_{88}H_{102}N_4Nd_2O_6$	$C_{60}H_{105}Al_2O_9Sm$
MW	1177.92	728.21	791.09	1600.22	1174.75
temp, K	203	203	203	203	203
space group	$P\bar{1}$	*Cmcm*	*Pbca*	$P2_1/c$	$P2_1/n$
a, Å	11.028(2)	11.304(2)	16.5822(9)	13.4496(8)	14.0960(7)
b, Å	12.168(2)	22.429(4)	15.5668(9)	20.034(1)	27.3037(15)
c, Å	12.879(2)	15.768(2)	29.902(2)	16.206(1)	16.7893(9)
α, deg	82.84(1)	90	90	90	90
β, deg	64.88(1)	90	90	113.782(1)	92.216(1)
γ, deg	70.80(1)	90	90	90	90
V, Å^3	1477.5(4)	3997.8(11)	7718.6(8)	3995.9(4)	6456.9(6)
Z	1	4	8	2	4
λ, Å	0.71073	0.71073	0.71073	0.71073	0.71073
D_{calcd}, g/mL	1.324	1.210	1.362	1.330	1.208
R1	0.0452	0.0582	0.0442	0.0298	0.0979
wR2	0.0956	0.1691	0.0885	0.0755	0.1659

[a] $R1 = \sum||F_o| - |F_c||/\sum|F_o|$ and $wR2 = [\sum[\omega(F_o^2 - F_c^2)^2]/\sum[\omega(F_o^2)^2]]^{1/2}$; $\omega = 1/[w^2(F_o^2) + (aP)^2]$, where $a = 0.0443$, 0.1078, 0.0353, 0.0308, and 0.0332.

atom positions. For **1**, one carbon atom position, C9, was disordered and modeled as two one-half occupancy positions. The structure of **2** was initially solved in space group $Cmc2_1$ using direct methods and difference Fourier techniques. The samarium, aluminum, and oxygen positions were revealed in the first difference map. The location of all carbon atom positions was not possible. The structure refinement stalled at $R1(4\sigma) = 0.1215$, with anisotropic temperature factors on metal and oxygen atoms only, and several unassigned carbon atom positions. At this point, a solution was obtained in space group *Cmcm*. All carbon atoms were located in subsequent difference maps. The terminal *tert*-butoxide and *iso*-butyl groups were disordered across and within mirror planes. The THF ligands were also disordered across a mirror plane. The disorder in the various ligands was modeled using several partial occupancy carbon and oxygen atoms. Soft restraints were placed on several ligand bond distances in order to obtain reasonable geometries. Because of the disorder of the ligands, hydrogen atom positions were not included in the model. The methyl hydrogen atom positions for C37 and C40 (**3**) were found on the difference map and refined with their isotropic temperature factors set to 0.08 Å^2. The methylene hydrogen atom positions for C41 and C43 (**4**) were also found and refined as described. All other hydrogen atom positions were idealized, C−H = 0.93 Å (aromatic), 0.96 Å (methyl), 0.98 Å (methine), and 0.97 Å (methylene). The hydrogen atoms were refined using a riding model, with isotropic temperature factors fixed at 1.5 (methyl) or 1.2 (all others) times the equivalent isotropic *U* of the atom they were bonded to. The final refinement[66] included anisotropic temperature factors on all atoms. Structure solution, refinement, graphics, and creation of publication materials were performed using SHELXTL 93 or NT.[67] Additional details of data collection and structure refinement are listed in Table 6.

Acknowledgment. We acknowledge the Office of Basic Energy Sciences, the Division of Chemical Sciences, and the U.S. Department of Energy for funding (via the LDRD ER program). K.J.Y. was the recipient of an Associated Western Universities Fellowship. Los Alamos National Laboratory is operated by the University of California for the U.S. Department of Energy under Contract W-7405-ENG-36.

Supporting Information Available: Crystallographic data in CIF format. This material is available free of charge via the Internet at http://pubs.acs.org.

IC0203116

(66) $R1 = \sum||F_o| - |F_c||/\sum|F_o|$ and $wR2 = [\sum[w(F_o^2 - F_c^2)^2]/\sum[\omega(F_o^2)^2]]^{1/2}$; $w = 1/[w^2(F_o^2) + (aP)^2]$, where $a = 0.0443$, 0.1078, 0.0353, 0.0308, and 0.0332.

(67) *SHELXTL* NT Version 5.10; Bruker Analytical X-ray Instruments, Inc.: Madison, WI, 1997.